

Study of B meson decays to three-body charmless hadronic final states

A. Garmash,^{2,9} K. Abe,⁹ K. Abe,⁴⁴ T. Abe,⁹ I. Adachi,⁹ H. Aihara,⁴⁶ M. Akatsu,²³ Y. Asano,⁵¹ T. Aushev,¹³ A. M. Bakich,⁴¹ Y. Ban,³⁴ I. Bedny,² P. K. Behera,⁵² I. Bizjak,¹⁴ A. Bondar,² A. Bozek,²⁸ M. Bračko,^{21,14} T. E. Browder,⁸ B. C. K. Casey,⁸ P. Chang,²⁷ Y. Chao,²⁷ K.-F. Chen,²⁷ B. G. Cheon,⁴⁰ R. Chistov,¹³ S.-K. Choi,⁷ Y. Choi,⁴⁰ A. Chuvikov,³⁵ M. Danilov,¹³ M. Dash,⁵³ L. Y. Dong,¹¹ A. Drutskoy,¹³ S. Eidelman,² V. Eiges,¹³ C. Fukunaga,⁴⁸ N. Gabyshev,⁹ T. Gershon,⁹ B. Golob,^{20,14} A. Gordon,²² R. Guo,²⁵ J. Haba,⁹ C. Hagner,⁵³ T. Hara,³² N. C. Hastings,⁹ H. Hayashii,²⁴ M. Hazumi,⁹ I. Higuchi,⁴⁵ L. Hinz,¹⁹ T. Hokuue,²³ Y. Hoshi,⁴⁴ W.-S. Hou,²⁷ H.-C. Huang,²⁷ Y. Igarashi,⁹ T. Iijima,²³ K. Inami,²³ R. Itoh,⁹ H. Iwasaki,⁹ M. Iwasaki,⁴⁶ Y. Iwasaki,⁹ H. K. Jang,³⁹ J. H. Kang,⁵⁵ J. S. Kang,¹⁶ N. Katayama,⁹ H. Kawai,³ T. Kawasaki,³⁰ H. Kichimi,⁹ D. W. Kim,⁴⁰ H. J. Kim,⁵⁵ Hyunwoo Kim,¹⁶ S. K. Kim,³⁹ K. Kinoshita,⁵ S. Korpar,^{21,14} P. Križan,^{20,14} P. Krokovny,² A. Kuzmin,² Y.-J. Kwon,⁵⁵ G. Leder,¹² S. H. Lee,³⁹ J. Li,³⁸ S.-W. Lin,²⁷ J. MacNaughton,¹² G. Majumder,⁴² F. Mandl,¹² H. Matsumoto,³⁰ A. Matyja,²⁸ W. Mitaroff,¹² H. Miyata,³⁰ G. R. Moloney,²² T. Mori,⁴⁷ Y. Nagasaka,¹⁰ T. Nakadaira,⁴⁶ E. Nakano,³¹ M. Nakao,⁹ J. W. Nam,⁴⁰ Z. Natkaniec,²⁸ S. Nishida,⁹ O. Nitoh,⁴⁹ T. Ohshima,²³ T. Okabe,²³ S. Okuno,¹⁵ S. L. Olsen,⁸ W. Ostrowicz,²⁸ H. Ozaki,⁹ H. Palka,²⁸ C. W. Park,¹⁶ H. Park,¹⁸ K. S. Park,⁴⁰ N. Parslow,⁴¹ L. E. Pilonen,⁵³ M. Rozanska,²⁸ H. Sagawa,⁹ S. Saitoh,⁹ Y. Sakai,⁹ T. R. Sarangi,⁵² M. Satapathy,⁵² A. Satpathy,^{9,5} O. Schneider,¹⁹ J. Schümann,²⁷ C. Schwanda,^{9,12} A. J. Schwartz,⁵ S. Semenov,¹³ K. Senyo,²³ R. Seuster,⁸ M. E. Sevier,²² H. Shibuya,⁴³ B. Shwartz,² V. Sidorov,² J. B. Singh,³³ N. Soni,³³ S. Stanić,^{51,*} M. Starič,¹⁴ A. Sugi,²³ K. Sumisawa,⁹ T. Sumiyoshi,⁴⁸ S. Suzuki,⁵⁴ S. Y. Suzuki,⁹ S. K. Swain,⁸ F. Takasaki,⁹ K. Tamai,⁹ N. Tamura,³⁰ J. Tanaka,⁴⁶ M. Tanaka,⁹ Y. Teramoto,³¹ T. Tomura,⁴⁶ K. Trabelsi,⁸ T. Tsuboyama,⁹ T. Tsukamoto,⁹ S. Uehara,⁹ Y. Unno,³ S. Uno,⁹ G. Varner,⁸ K. E. Varvell,⁴¹ C. H. Wang,²⁶ M.-Z. Wang,²⁷ Y. Watanabe,⁴⁷ E. Won,¹⁶ B. D. Yabsley,⁵³ Y. Yamada,⁹ A. Yamaguchi,⁴⁵ H. Yamamoto,⁴⁵ Y. Yamashita,²⁹ M. Yamauchi,⁹ H. Yanai,³⁰ Y. Yuan,¹¹ Y. Yusa,⁴⁵ J. Zhang,⁵¹ Z. P. Zhang,³⁸ V. Zhilich,² and D. Zontar^{20,14}

(Belle Collaboration)

¹Aomori University, Aomori²Budker Institute of Nuclear Physics, Novosibirsk³Chiba University, Chiba⁴Chuo University, Tokyo⁵University of Cincinnati, Cincinnati, Ohio 45221⁶University of Frankfurt, Frankfurt⁷Gyeongsang National University, Chinju⁸University of Hawaii, Honolulu, Hawaii 96822⁹High Energy Accelerator Research Organization (KEK), Tsukuba¹⁰Hiroshima Institute of Technology, Hiroshima¹¹Institute of High Energy Physics, Chinese Academy of Sciences, Beijing¹²Institute of High Energy Physics, Vienna¹³Institute for Theoretical and Experimental Physics, Moscow¹⁴J. Stefan Institute, Ljubljana¹⁵Kanagawa University, Yokohama¹⁶Korea University, Seoul¹⁷Kyoto University, Kyoto¹⁸Kyungpook National University, Taegu¹⁹Institut de Physique des Hautes Énergies, Université de Lausanne, Lausanne²⁰University of Ljubljana, Ljubljana²¹University of Maribor, Maribor²²University of Melbourne, Victoria²³Nagoya University, Nagoya²⁴Nara Women's University, Nara²⁵National Kaohsiung Normal University, Kaohsiung²⁶National Lien-Ho Institute of Technology, Miao Li²⁷Department of Physics, National Taiwan University, Taipei²⁸H. Niewodniczanski Institute of Nuclear Physics, Krakow²⁹Nihon Dental College, Niigata³⁰Niigata University, Niigata³¹Osaka City University, Osaka³²Osaka University, Osaka³³Panjab University, Chandigarh³⁴Peking University, Beijing³⁵Princeton University, Princeton, New Jersey 08545

³⁶RIKEN BNL Research Center, Upton, New York 11973³⁷Saga University, Saga³⁸University of Science and Technology of China, Hefei³⁹Seoul National University, Seoul⁴⁰Sungkyunkwan University, Suwon⁴¹University of Sydney, Sydney NSW⁴²Tata Institute of Fundamental Research, Bombay⁴³Toho University, Funabashi⁴⁴Tohoku Gakuin University, Tagajo⁴⁵Tohoku University, Sendai⁴⁶Department of Physics, University of Tokyo, Tokyo⁴⁷Tokyo Institute of Technology, Tokyo⁴⁸Tokyo Metropolitan University, Tokyo⁴⁹Tokyo University of Agriculture and Technology, Tokyo⁵⁰Toyama National College of Maritime Technology, Toyama⁵¹University of Tsukuba, Tsukuba⁵²Utkal University, Bhubaneswar⁵³Virginia Polytechnic Institute and State University, Blacksburg, Virginia 24061⁵⁴Yokkaichi University, Yokkaichi⁵⁵Yonsei University, Seoul

(Received 1 August 2003; published 9 January 2004)

We report results of a study of charmless B meson decays to three-body $K\pi\pi$, $KK\pi$ and KKK final states. Measurements of branching fractions for B decays to $K^{+(0)}\pi^+\pi^-$, $K^+K^+K^-$, $K^0K^+K^-$, $K^+K_S^0K_S^0$ and $K_S^0K_S^0K_S^0$ final states are presented. The decays $B^0 \rightarrow K^0K^+K^-$, $B^+ \rightarrow K^+K_S^0K_S^0$ and $B^0 \rightarrow K_S^0K_S^0K_S^0$ are observed for the first time. We also report evidence for $B^+ \rightarrow K^+K^-\pi^+$ decay. For the three-body final states $K^0K^+\pi^-$, $K_S^0K_S^0\pi^+$, $K^+K^+\pi^-$ and $K^-\pi^+\pi^+$, 90% confidence level upper limits are reported. Finally, we discuss the possibility of using the three-body $B^0 \rightarrow K_S^0K^+K^-$ decay for CP violation studies. The results are obtained with a 78 fb^{-1} data sample collected at the $\Upsilon(4S)$ resonance by the Belle detector operating at the KEKB asymmetric energy e^+e^- collider.

DOI: 10.1103/PhysRevD.69.012001

PACS number(s): 13.25.Hw, 14.40.Nd

I. INTRODUCTION

Studies of three-body charmless hadronic final states are a natural extension of studies of two-body final states. Some of the final states considered so far as two-body (for example $\rho\pi$, $K^*\pi$, etc.) are, in fact, quasi-two-body since they produce a wide resonance state that immediately decays, in the simplest case, into two particles producing a three-body final state. Multiple resonances occurring nearby in phase space will interfere and a full amplitude analysis is required to extract correct branching fractions for the intermediate quasi-two-body states. B meson decays to three-body charmless hadronic final states may also provide new possibilities for CP violation searches. For example, a new method to extract the weak angle ϕ_3 from isospin analysis and measurement of time dependent asymmetry in the decay $B^0 \rightarrow K_S^0\pi^+\pi^-$ has been recently suggested in Ref. [1]. Charmless decays of B mesons are also important in current searches for physics beyond the standard model (SM). Among three-body charmless final states, the $B^+ \rightarrow K^+K^+\pi^-$ and $B^+ \rightarrow K^-\pi^+\pi^+$ decays, which proceed via $b \rightarrow ss\bar{d}$ and $b \rightarrow dd\bar{s}$ transitions, respectively, provide a good opportunity to search for new

physics. The SM prediction for the branching fraction of the decay $B^+ \rightarrow K^+K^+\pi^-$ is of order 10^{-11} and even smaller for the $K^-\pi^+\pi^+$ final state [2]. However, there are extensions of the SM where these branching fractions can be enhanced up to 10^{-7} [2,3]. Upper limits on branching fractions for these final states can be used to constrain parameters in some extensions of the SM [4].

B meson decays to $K^{+(0)}\pi^+\pi^-$ and $K^+K^+K^-$ final states have already been observed by the Belle, BaBar and CLEO experiments [5–7]. For the other three-body charmless hadronic final states considered in this paper only upper limits have been reported so far [8]. In this paper, we present updated results on a study of B meson decays to three-body $K\pi\pi$, $KK\pi$ and KKK final states. We also describe an isospin analysis of the decays of B mesons to three-kaon final states and discuss the use of the $B^0 \rightarrow K_S^0K^+K^-$ three-body decay for CP violation measurements.

The analysis is based on a 78 fb^{-1} data sample, which contains 85.0 million $B\bar{B}$ pairs, collected with the Belle detector operating at the KEKB asymmetric-energy e^+e^- collider [9] with a center-of-mass (c.m.) energy at the $\Upsilon(4S)$ resonance. The beam energies are 3.5 GeV for positrons and 8.0 GeV for electrons. For the study of the $e^+e^- \rightarrow q\bar{q}$ continuum background we use 8.3 fb^{-1} of data taken 60 MeV below the $\Upsilon(4S)$ resonance. The results presented here in-

*On leave from Nova Gorica Polytechnic, Nova Gorica.

clude the previous data and supersede the results on three-body charmless hadronic final states reported in Ref. [5].

II. THE BELLE DETECTOR

The Belle detector [10] is a large-solid-angle magnetic spectrometer based on a 1.5 T superconducting solenoid magnet. Charged particle tracking is provided by a three-layer silicon vertex detector and a 50-layer central drift chamber (CDC) that surround the interaction point. The charged particle acceptance covers the laboratory polar angle between $\theta = 17^\circ$ and 150° , corresponding to about 92% of the full solid angle in the c.m. frame. The momentum resolution is determined from cosmic rays and $e^+e^- \rightarrow \mu^+\mu^-$ events to be $\sigma_{p_t}/p_t = (0.30 \oplus 0.19 p_t)\%$, where p_t is the transverse momentum in GeV/c.

Charged hadron identification is provided by dE/dx measurements in the CDC, an array of 1188 aerogel Čerenkov counters (ACC), and a barrel-like array of 128 time-of-flight scintillation counters (TOF); information from the three sub-detectors is combined to form a single likelihood ratio, which is then used in kaon and pion selection. At large momenta (> 2.5 GeV/c) only the ACC and CDC are used to separate charged pions and kaons since here the TOF provides no additional discrimination. Electromagnetic showering particles are detected in an array of 8736 CsI(Tl) crystals that covers the same solid angle as the charged particle tracking system. The energy resolution for electromagnetic showers is $\sigma_E/E = (1.3 \oplus 0.07/E \oplus 0.8/E^{1/4})\%$, where E is in GeV. Electron identification in Belle is based on a combination of dE/dx measurements in the CDC, the response of the ACC, and the position, shape and total energy deposition (i.e., E/p) of the shower detected in the calorimeter. The electron identification efficiency is greater than 92% for tracks with $p_{\text{lab}} > 1.0$ GeV/c and the hadron misidentification probability is below 0.3%. The magnetic field is returned via an iron yoke that is instrumented to detect muons and K_L^0 mesons. We use a GEANT-based Monte Carlo (MC) simulation to model the response of the detector and determine acceptance [11].

III. EVENT SELECTION

Charged tracks are selected with a set of track quality requirements based on the average hit residual and on the distances of closest approach to the interaction point (IP). We also require that the track momenta transverse to the beam be greater than 0.1 GeV/c to reduce the low momentum combinatorial background. For charged kaon identification, we impose a requirement on the particle identification variable, which has 86% efficiency and a 7% fake rate from misidentified pions. Charged tracks that are positively identified as electrons or protons are excluded. Since the muon identification efficiency and fake rate vary significantly with the track momentum, we do not veto muons to avoid additional systematic errors.

Neutral kaons are reconstructed via the decay $K^0(\bar{K}^0) \rightarrow \pi^+\pi^-$. The invariant mass of the two pions is required to be within 12 MeV/c² of the nominal K^0 mass. The displace-

ment of the $\pi^+\pi^-$ vertex from the IP in the r - ϕ plane is required to be greater than 0.1 cm and less than 20 cm. The direction of the combined pion pair momentum in the r - ϕ plane must be within 0.2 rad of the direction from the IP to the displaced vertex.

We reconstruct B mesons in three-body $K\pi\pi$, $KK\pi$ and KKK final states, where K stands for a charged or neutral kaon, and π for a charged pion. The inclusion of the charge conjugate mode is implied throughout this paper. The candidate events are identified by their c.m. energy difference, $\Delta E = (\sum_i E_i) - E_{\text{beam}}$, and the beam constrained mass, $M_{\text{bc}} = \sqrt{E_{\text{beam}}^2 - (\sum_i \vec{p}_i)^2}$, where $E_{\text{beam}} = \sqrt{s}/2$ is the beam energy in the c.m. frame, and \vec{p}_i and E_i are the c.m. three-momenta and energies of the candidate B meson decay products. We select events with $M_{\text{bc}} > 5.20$ GeV/c² and $-0.30 < \Delta E < 0.50$ GeV. For subsequent analysis, we also define a M_{bc} signal region of $|M_{\text{bc}} - M_B| < 9$ MeV/c².

To determine the signal yield, we use events with M_{bc} in the signal region and fit the ΔE distribution with the sum of a signal and a background function. The ΔE signal is parametrized by the sum of two Gaussian functions with the same mean. The widths and the relative fractions of the two Gaussians are determined from the MC simulation. We find that the signal MC events have a 10% narrower ΔE width than seen in the data. To correct for this effect, we introduce a scale factor that is determined from the comparison of the ΔE widths for $B^+ \rightarrow \bar{D}^0 \pi^+$ events in MC and experimental data. The ΔE shape of the $B\bar{B}$ produced background is determined from MC simulation, as described below. The background from $e^+e^- \rightarrow q\bar{q}$ ($q = u, d, s$ and c quarks) continuum events is represented by a linear function.

IV. BACKGROUND SUPPRESSION

An important issue for this analysis is the suppression of the large combinatorial background, which is dominated by $q\bar{q}$ continuum events. We suppress this background using variables that characterize the event topology. A more detailed description of the background suppression technique can be found in Ref. [5].

Since the two B mesons produced from an $Y(4S)$ decay are nearly at rest in the c.m. frame, their decay products are uncorrelated and events tend to be spherical. In contrast, hadrons from continuum $q\bar{q}$ events tend to exhibit a two-jet structure. We use θ_{thr} , which is the angle between the thrust axis of the B candidate and that of the rest of the event, to discriminate between the two cases. The distribution of $|\cos\theta_{\text{thr}}|$, shown in Fig. 1(a), is strongly peaked near $|\cos\theta_{\text{thr}}| = 1.0$ for $q\bar{q}$ events and is nearly flat for $B\bar{B}$ events. We require $|\cos\theta_{\text{thr}}| < 0.80$ for all three-body final states; this eliminates about 83% of the continuum background and retains 79% of the signal events.

After imposing the $\cos\theta_{\text{thr}}$ requirement, the remaining $q\bar{q}$ and $B\bar{B}$ events still have some differences in topology that

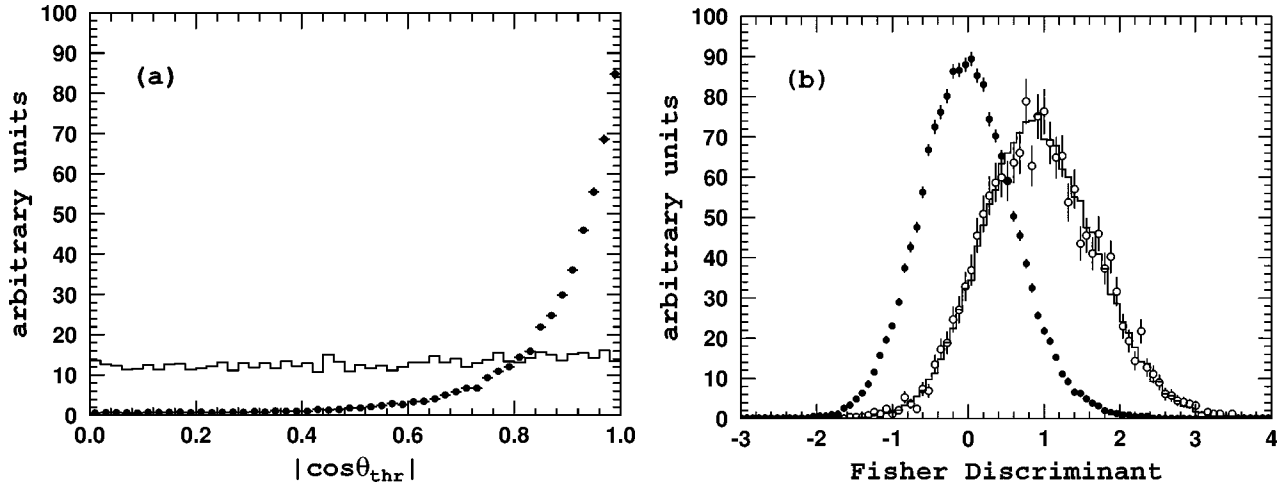


FIG. 1. Distribution of (a) $|\cos\theta_{\text{thr}}|$ and (b) Fisher discriminant for the $B^+ \rightarrow K^+ \pi^+ \pi^-$ signal MC events (histogram), $B^+ \rightarrow \bar{D}^0 \pi^+$ events in data (open circles) and $q\bar{q}$ background in below-resonance data (filled circles).

are exploited for further continuum suppression. A Fisher discriminant [12] is formed from 11 variables: nine variables that characterize the angular distribution of the momentum flow in the event with respect to the B candidate thrust axis [13], the angle of the B candidate thrust axis with respect to the beam axis, and the angle between the B candidate momentum and the beam axis. The discriminant, \mathcal{F} , is the linear combination of the input variables that maximizes the separation between signal and background. The coefficients are determined using below-resonance data and a large set of $B^+ \rightarrow K^+ \pi^+ \pi^-$ signal MC events. We use the same set of coefficients for all three-body final states. Figure 1(b) compares the \mathcal{F} distributions for the $B^+ \rightarrow K^+ \pi^+ \pi^-$ signal MC events, $B^+ \rightarrow \bar{D}^0 \pi^+$ events in data and $q\bar{q}$ background events in below-resonance data. The separation between the mean values of the discriminant for the signal and background is approximately 1.3 times the signal width. For all $K\pi\pi$ and $KK\pi$ final states we impose a requirement $\mathcal{F} > 0.8$ on the Fisher discriminant variable that rejects about 90% of the remaining continuum background and retains 54% of the signal. The continuum background in the three-kaon final states is much smaller and a looser requirement $\mathcal{F} > 0$ is imposed to retain the efficiency. This requirement rejects 53% of the remaining $q\bar{q}$ background and retains 89% of the signal.

We also consider backgrounds that come from other B decays. We subdivide this background into two types. The first type is the background from decays that are dominantly $b \rightarrow c$ tree transition. The description of these decays is taken from an updated version of the CLEO group event generator [14]. The other potential source of background is charmless B decays that proceed via $b \rightarrow s(d)$ penguins or $b \rightarrow u$ tree transitions. We studied a large set of potentially serious backgrounds from two-, three-, and four-body final states. Since the background from other B decays is substantially mode dependent, we give a detailed description of this type of background for each final state in the following sections.

V. $B^{+(0)} \rightarrow K^{+(0)} \pi^+ \pi^-$

We find that the dominant background to the $K^{+(0)} \pi^+ \pi^-$ final states from other B decays is due to the $B \rightarrow D\pi$, $D \rightarrow K\pi$ decays and due to $B^+ \rightarrow J/\psi[\psi(2S)]K^+$ decays, where $J/\psi[\psi(2S)] \rightarrow \mu^+ \mu^-$. To exclude the $B \rightarrow D\pi$ events, we apply the requirement on the $K\pi$ invariant mass $|M(K\pi) - M_D| > 0.10 \text{ GeV}/c^2$, where M_D is the world average value for mass of the $D^{0(+)}$ meson [8]. To suppress the background due to π/K misidentification in the $K^+ \pi^+ \pi^-$ final state, we also exclude candidates if the invariant mass of any pair of oppositely charged tracks from the B candidate is consistent with the $\bar{D}^0 \rightarrow K^+ \pi^-$ hypothesis within $15 \text{ MeV}/c^2$ ($\sim 2.5\sigma$), independently of the particle identification information. Modes with a $J/\psi[\psi(2S)]$ in the final state contribute due to muon-pion misidentification; the contribution from the $J/\psi[\psi(2S)] \rightarrow e^+ e^-$ submode is found to be negligible (less than 0.5%) after the electron veto requirement. We exclude $J/\psi[\psi(2S)]$ signals by requiring $|M(h^+ h^-) - M_{J/\psi}| > 0.07 \text{ GeV}/c^2$ and $|M(h^+ h^-) - M_{\psi(2S)}| > 0.05 \text{ GeV}/c^2$, where h^+ and h^- are pion candidates [15]. Finally, we also reject candidates if the $\pi^+ \pi^-$ invariant mass is within $50 \text{ MeV}/c^2$ of the world average χ_{c0} mass [8]. The most significant background from charmless B decays is found to originate from the $B^{+(0)} \rightarrow \eta' K^{+(0)}$ followed by $\eta' \rightarrow \pi^+ \pi^- \gamma$ decays. Another contribution comes from the $B^+ \rightarrow \rho^0 \pi^+$ final state, where one of the final state pions is misidentified as a kaon. There is also a background from two-body charmless $B \rightarrow K\pi$ decays. Although this background is shifted by about 0.2 GeV from the ΔE signal region, it is important to take it into account to estimate correctly the background from $q\bar{q}$ continuum events.

The ΔE distributions for selected $B^{+(0)} \rightarrow K^{+(0)} \pi^+ \pi^-$ candidates that pass all the selection requirements are shown in Fig. 2. A significant enhancement in the B signal region is observed for both final states. Results of the fits are shown as open histograms in Fig. 2 and hatched histograms represent

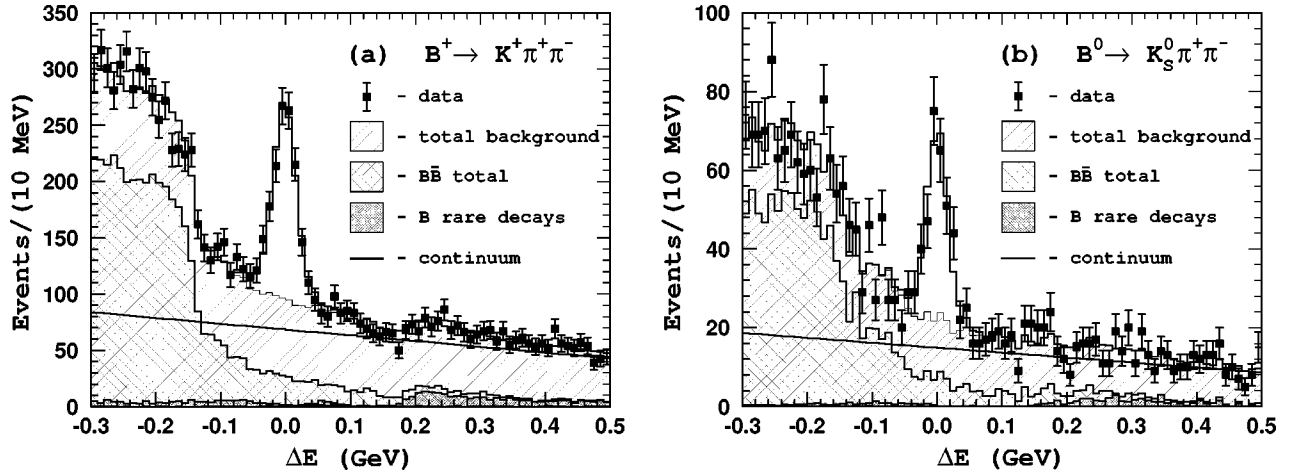


FIG. 2. ΔE distributions for (a) $B^+ \rightarrow K^+ \pi^+ \pi^-$ and (b) $B^0 \rightarrow K^0 \pi^+ \pi^-$. Points with error bars represent data, the open histogram is the result of the fit, and the hatched histogram shows the total background level. The straight line indicates the $q\bar{q}$ continuum background contribution.

the background. While fitting the data we fix the shape of the $B\bar{B}$ background and allow its normalization to float. For background from charmless B decays we fix the normalization as well. Both the normalization and the slope of the $q\bar{q}$ background are floated during the fit. There is a large increase in the level of the $B\bar{B}$ related background in the $\Delta E < -0.15$ GeV region that is mainly due to $B \rightarrow D\pi$, $D \rightarrow K\pi\pi$ decays. This decay mode produces the same final state as the studied process plus one extra pion that is not included in the energy difference calculation. The decay $B \rightarrow D\pi$, $D \rightarrow K\mu\nu_\mu$ also contributes due to muon-pion mis-

identification. The shape of this background is well described by MC simulation. The signal yields from fits are given in Table I.

VI. $B \rightarrow KKK$

The dominant background from other B decays to the three-kaon final states is from $B \rightarrow Dh$ decays, where h stands for a charged pion or kaon. To suppress this background, we reject events where the two-particle invariant mass is consistent within $15 \text{ MeV}/c^2$ ($\sim 2.5\sigma$) with $D^0 \rightarrow K^+ K^-$ for the $K^+ K^+ K^-$ final state and with D^+

TABLE I. Summary of results for B meson decays to three-body charmless hadronic final states. The table lists the three-body decay modes, the corresponding ΔE resolution for the core (σ_1) and the tail (σ_2) Gaussian functions, the fraction of the signal in the core Gaussian, three-body reconstruction efficiency, the signal yield extracted from the ΔE fit and branching fractions. The branching fractions and 90% confidence level (C.L.) upper limits (UL) are quoted in units of 10^{-6} . For the modes with neutral kaons the quoted reconstruction efficiencies include the intermediate branching fractions. Two values for the $B \rightarrow D\pi$ efficiency and signal yield correspond to $\mathcal{F} > 0.8$ (> 0) requirement on the Fisher discriminant.

Three-body mode	ΔE resolution σ_1/σ_2 (MeV)	Fraction	Efficiency (%)	Signal Yield (events)	\mathcal{B} or 90% C.L. UL (10^{-6})
$K^+ \pi^+ \pi^-$	17.3/35.0	0.85	21.5 ± 0.48	845 ± 46	$53.6 \pm 3.1 \pm 5.1$
$K^0 \pi^+ \pi^-$	15.2/40.0	0.85	5.85 ± 0.11	209 ± 21	$45.4 \pm 5.2 \pm 5.9$
$K^+ K^+ K^-$	14.5/40.0	0.85	23.5 ± 0.50	565 ± 30	$32.8 \pm 1.8 \pm 2.8$
$K^0 K^+ K^-$	14.0/40.0	0.85	7.20 ± 0.17	149 ± 15	$28.3 \pm 3.3 \pm 4.0$
$K^+ K_S^0 K_S^0$	14.3/40.0	0.85	6.78 ± 0.19	66.5 ± 9.3	$13.4 \pm 1.9 \pm 1.5$
$K_S^0 K_S^0 K_S^0$	14.7/40.0	0.85	3.98 ± 0.17	$12.2^{+4.5}_{-3.8}$	$4.2^{+1.6}_{-1.3} \pm 0.8$
$K^+ K^- \pi^+$	15.5/40.0	0.85	13.8 ± 0.31	94 ± 23 (< 130)	$9.3 \pm 2.3 \pm 1.1$ (< 13)
$K^0 K^+ \pi^-$	14.7/40.0	0.85	4.53 ± 0.16	27 ± 17 (< 55)	< 18
$K_S^0 K_S^0 \pi^+$	15.0/40.0	0.85	5.31 ± 0.15	-1.8 ± 7.7 (< 11)	< 3.2
$K^- \pi^+ \pi^+$	17.0/40.0	0.85	17.0 ± 0.37	21 ± 18 (< 51)	< 4.5
$K^+ K^+ \pi^-$	15.5/40.0	0.85	14.2 ± 0.30	6.5 ± 9.6 (< 22.3)	< 2.4
$\bar{D}^0 \pi^+$	14.5/30.0	0.80	17.8 ± 0.43 (28.8 ± 0.57)	2470 ± 51 (4000 ± 66)	
$D^- \pi^+$	14.9/40.0	0.80	5.10 ± 0.11 (8.24 ± 0.14)	300 ± 16 (451 ± 25)	

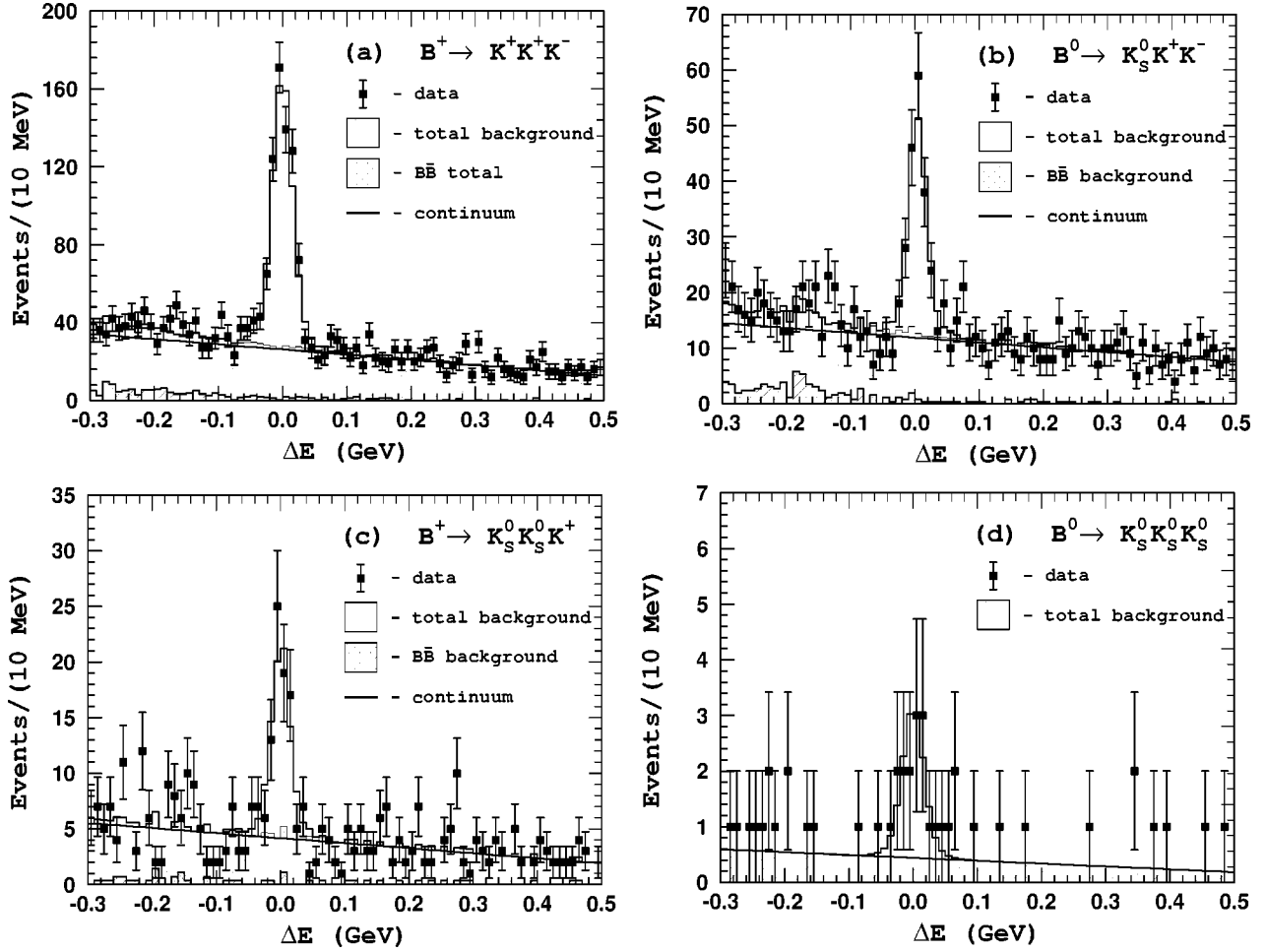


FIG. 3. ΔE distributions for $B \rightarrow KKK$ three-body final states. Points with error bars are data; the open histogram is the fit result; the hatched histogram is the background. The straight line shows the $q\bar{q}$ continuum background contribution.

$\rightarrow \bar{K}^0 K^+$ for the $K^0 K^+ K^-$ final state. To suppress the background due to π/K misidentification in the $K^+ K^+ K^-$ final state, we also exclude candidates if the invariant mass of any pair of oppositely charged tracks from the B candidate is consistent with $D^0 \rightarrow K^- \pi^+$ within $15 \text{ MeV}/c^2$ ($\sim 2.5\sigma$), independently of the particle identification information. For the $K^0 K^+ K^-$ final state we exclude candidates if the $K_S^0 h^\pm$ invariant mass is consistent with $D^+ \rightarrow \bar{K}^0 \pi^+$ within $15 \text{ MeV}/c^2$. We also reject events with a $K^+ K^-$ invariant mass that is consistent with $\chi_{c0} \rightarrow K^+ K^-$ within $50 \text{ MeV}/c^2$. We do not find any charmless B decay modes that produce a significant background to the three-kaon final states. The feed-across between $K^{+(0)} \pi^+ \pi^-$ and $K^{+(0)} K^+ K^-$ final states is also found to be negligible.

The ΔE distributions for all three-kaon final states are shown in Fig. 3, where data (points with error bars) are shown along with the expected background (hatched histograms). The $B\bar{B}$ background in KKK final states is much smaller than that in the $K^{+(0)} \pi^+ \pi^-$ final states and has no prominent structures. The results of fits to the ΔE distributions are summarized in Table I. While fitting the data for all three-kaon final states we fix not only the shape but also the normalization of the $B\bar{B}$ related background. The statistical

significance of the $B^0 \rightarrow K_S^0 K_S^0 K_S^0$ signal, in terms of the number of standard deviations is 4.3σ . It is calculated as $\sqrt{-2\ln(\mathcal{L}_0/\mathcal{L}_{\max})}$, where \mathcal{L}_{\max} and \mathcal{L}_0 denote the maximum likelihood with the nominal signal yield and with the signal yield fixed at zero, respectively. The significance of the signal in all other three-kaon final states exceeds 10σ .

VII. $B^{+(0)} \rightarrow K^{+(0)} K^- \pi^+$, $K_S^0 K_S^0 \pi^+$, $K^+ K^+ \pi^-$ AND $K^- \pi^+ \pi^+$

The signals in the $K^{+(0)} K^- \pi^+$ and $K_S^0 K_S^0 \pi^+$ channels are, in general, expected to be much smaller since the dominant contributions to these final states are expected to come from the $b \rightarrow u$ tree and $b \rightarrow dg$ penguin transitions, while the $B^{+(0)} \rightarrow K^{+(0)} \pi^+ \pi^-$ and $B \rightarrow KKK$ decay channels are dominantly $b \rightarrow sg$ penguin transitions. As for the $B^+ \rightarrow K^+ K^+ \pi^-$ and $B^+ \rightarrow K^- \pi^+ \pi^+$ decays, the SM predicts exceedingly small branching fractions for these decays (as mentioned above).

The background from other B meson decays to these final states is mainly due to $B \rightarrow Dh$ decays, where h represents a charged pion or kaon. We suppress this background by rejecting events where the two-particle invariant mass is consistent within $15 \text{ MeV}/c^2$ ($\sim 2.5\sigma$) with $D^0 \rightarrow K^+ K^-$, D^0

$\rightarrow K^- \pi^+$, $D^+ \rightarrow \bar{K}^0 \pi^+$ or $D^+ \rightarrow \bar{K}^0 K^+$. Because of the small expected signal to background ratio for these final states, a different technique for signal yield extraction is used. We subdivide the ΔE region into 20 MeV bins and determine the signal yield in each bin from the fit to the corresponding M_{bc} spectrum. The M_{bc} signal shape is parametrized by a Gaussian function. The width of the M_{bc} signal is primarily due to the c.m. energy spread and is expected to be the same for each decay channel; in the fit we fix it at the value $\sigma_{M_{bc}} = 3.0 \text{ MeV}/c^2$ determined from the $B^+ \rightarrow \bar{D}^0 \pi^+$, $\bar{D}^0 \rightarrow K^+ \pi^-$ events in the same data sample. The background shape is parametrized with the empirical function $f(M_{bc}) \propto x \sqrt{1-x^2} \exp[-\xi(1-x^2)]$, where $x = M_{bc}/E_{\text{beam}}$ and ξ is a parameter [16]. We fix the ξ value from a study of data taken below the $Y(4S)$ resonance. The signal yield from the M_{bc} fit as a function of ΔE is used in the subsequent analysis. Since the $q\bar{q}$ background does not peak in the M_{bc} distribution, this technique allows an effective subtraction of the $q\bar{q}$ background. In contrast, the $B\bar{B}$ background can easily produce a signal-like distribution in the M_{bc} variable. The same procedure is applied to the $B\bar{B}$ MC events to determine the background shape and level. The resulting continuum-background-subtracted ΔE distributions are fit with the signal yield as the only free parameter. Figure 4 shows the results of the fit, along with the expected contributions from generic $B\bar{B}$ decays and the feed-down due to particle misidentification from the $B \rightarrow K\pi\pi$ and $B \rightarrow KKK$ decay modes. For the $K^- \pi^+ \pi^+$ final state, shown in Fig. 4(a), the only background from charmless B decays is due to $\bar{B}^0 \rightarrow K^- \pi^+$ two-body decay. For the $K^+ K^- \pi^+$ final state, shown in Fig. 4(c), we observe an excess of events in the signal region with statistical significance of 4σ . For all other final states presented in Fig. 4, the experimental points are consistent with the background expectations.

VIII. BRANCHING FRACTION CALCULATION

To determine branching fractions, we normalize our results to the observed $B^+ \rightarrow \bar{D}^0 \pi^+$, $\bar{D}^0 \rightarrow K^+ \pi^-$ and $B^0 \rightarrow D^- \pi^+$, $D^- \rightarrow K^0 \pi^-$ signals. This reduces the systematic errors associated with the charged track reconstruction efficiency, particle identification efficiency, the event shape variables and uncertainty due to the possible nonuniform data taking conditions during the experiment. We calculate the branching fraction for B meson decay to a particular final state f via the relation

$$\mathcal{B}(B \rightarrow f) = \frac{N_f}{N_{D\pi}} \frac{\varepsilon_{D\pi}}{\varepsilon_f} \times \mathcal{B}(B \rightarrow D\pi) \mathcal{B}(D \rightarrow K\pi), \quad (1)$$

where N_f and $N_{D\pi}$ are the number of reconstructed signal events for the final state f and that for the $D\pi$ reference process, and ε_f and $\varepsilon_{D\pi}$ are the corresponding reconstruction efficiencies determined from MC. The $B \rightarrow D\pi$ and $D \rightarrow K\pi$ branching fractions are the world average values from the PDG [8].

To select $B \rightarrow D\pi$ events, we require that the $K\pi$ invariant mass be consistent within 3σ with the D meson nominal mass [8]. The ΔE distributions for the reference processes $B^+ \rightarrow \bar{D}^0 \pi^+$, $\bar{D}^0 \rightarrow K^+ \pi^-$ and $B^0 \rightarrow D^- \pi^+$, $D^- \rightarrow K^0 \pi^-$ are shown in Fig. 5. The results of the fits are given in Table I. Since, in the analysis of $K\pi\pi$ ($KK\pi$) and KKK final states, different requirements on the Fisher discriminant are applied, we determine the $B \rightarrow D\pi$ signal yields for these two cases.

The results of the three-body branching fraction measurements are presented in Table I. To determine the reconstruction efficiencies for $K^+ K^+ K^-$ and $K^0 K^+ K^-$ final states, we use a simple model [5] that takes into account the nonuniform distribution of signal events over the Dalitz plot. The three-body signal in this model is parametrized by a ϕK intermediate state and a $f_X K$ state, where f_X is a hypothetical wide scalar state. Another model is used for the $K^{+(0)} \pi^+ \pi^-$ final states to account for the nonuniform distribution of signal events over the Dalitz plot and determine the reconstruction efficiencies [5]. The three-body $K^{+(0)} \pi^+ \pi^-$ signal in this model is parametrized by the following set of quasi-two-body intermediate states: $\rho^0 K$, $f_0(980)K$, $K^*(892)\pi$, $K_0^*(1430)\pi$ and $f_0(1370)\pi$. For the $K^- \pi^+ \pi^+$, $K^+ K_S^0 K_S^0$, $K_S^0 K_S^0 K_S^0$ and all $KK\pi$ final states, the reconstruction efficiency is determined from MC simulated events that are generated with a uniform (phase space) distribution over the Dalitz plot. For the $B^+ \rightarrow K^+ K^- \pi^+$ decay the statistical significance of the signal barely exceeds 4σ and as a final result we set a 90% confidence level upper limit on its branching fraction, though the central value is also given in Table I. Since we do not observe a statistically significant signal in any of the $K^- \pi^+ \pi^+$, $K^+ K^+ \pi^-$, $K^0 K^+ \pi^-$ and $K_S^0 K_S^0 \pi^+$ final states, we place 90% confidence level upper limits on their branching fractions [17]. These limits are given in Table I. To take into account the systematic uncertainty, we reduce the reconstruction efficiency by one standard deviation of the overall systematic error.

The dominant sources of systematic error are listed in Table II. For the $B^{+(0)} \rightarrow K^{+(0)} \pi^+ \pi^-$ and $B^{+(0)} \rightarrow K^{+(0)} K^+ K^-$ final states, we estimate the systematic uncertainty due to variations of reconstruction efficiency over the Dalitz plot by varying the relative phases of quasi-two-body states in the range from 0 to 2π and their amplitudes within $\pm 20\%$. For all other final states we make a conservative estimate of this type of systematic uncertainty. For each three-body final state the Dalitz plot is subdivided in $2 \text{ GeV}^2/c^4$ wide slices in $M^2(hh)$ [for example $M^2(K^- \pi^+)$ for the $K^+ K^- \pi^+$ final state], and the reconstruction efficiency is determined in each bin. The same procedure is then applied for the second Dalitz plot projection [$M^2(K^+ K^-)$ for the $B^+ \rightarrow K^+ K^- \pi^+$ decay]. The maximal variation in the reconstruction efficiency for all bins is taken as the systematic error. The uncertainty due to the particle identification is estimated using high purity samples of kaons and pions from the $D^0 \rightarrow K^- \pi^+$ decays, where the D^0 flavor is tagged using $D^{*+} \rightarrow D^0 \pi^+$ decays. The systematic error due to uncertainty in the K_S^0 reconstruction efficiency is estimated from the comparison of the relative yields of inclusive K_S^0 's in

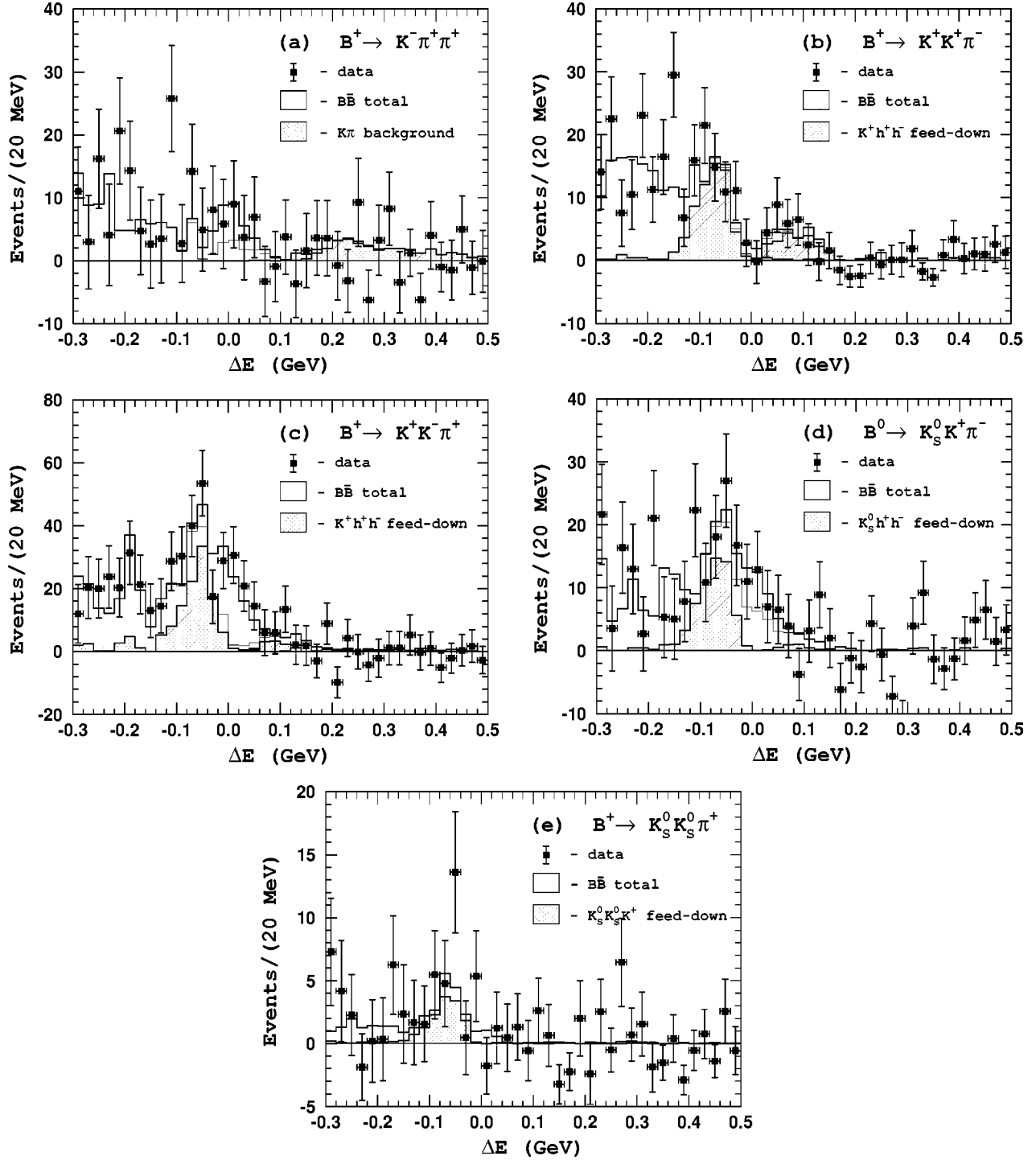


FIG. 4. Results of the fit (open histogram) to the M_{bc} distributions in ΔE bins. The data (points with error bars) are compared with the $B\bar{B}$ MC expectation (hatched histogram). The feed-down from KKK and $K\pi\pi$ final states is shown by filled histograms.

off-resonance data and $q\bar{q}$ MC with variation of the K_S^0 selection criteria. We estimate the uncertainty due to the signal ΔE shape parametrization by allowing the width of the main Gaussian function to float and varying other parameters of the fitting function within their errors. The uncertainty in the background parametrization is estimated by varying the relative fractions of the background components and parameters of the $q\bar{q}$ background shape function within their errors. The

overall systematic uncertainty for the three-body branching fractions varies from 9% to 18%, as given in Table II.

IX. IMPLICATION FOR CP VIOLATION STUDY

An important check of the standard model would be provided by measurements of the same CP -violating parameter in different weak interaction processes. A good example is

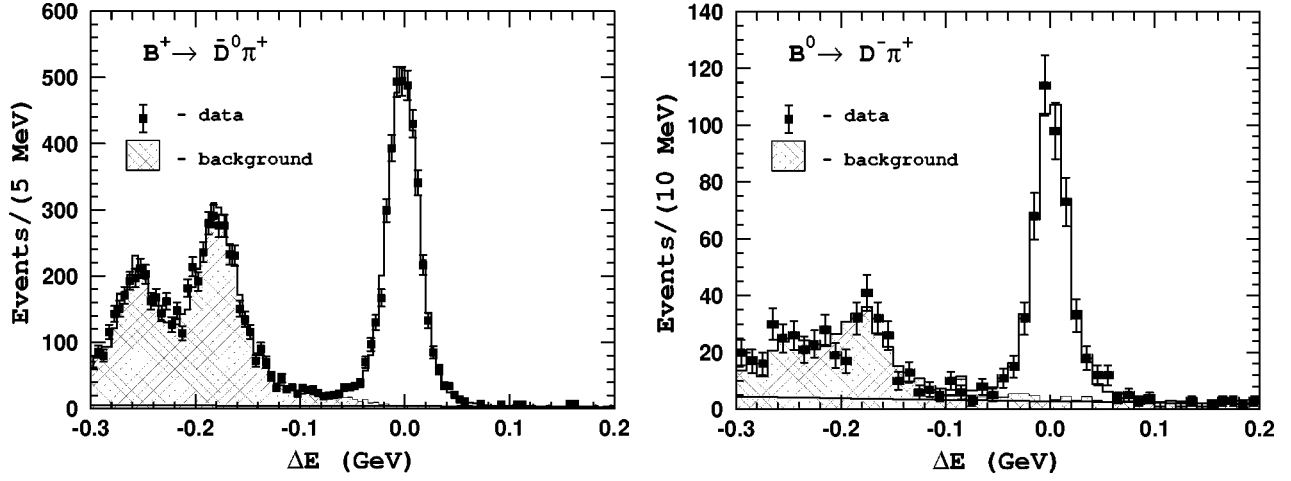


FIG. 5. ΔE distributions for $B^+ \rightarrow \bar{D}^0 \pi^+$, $\bar{D}^0 \rightarrow K^+ \pi^-$ (left) and $B^0 \rightarrow D^- \pi^+$, $D^- \rightarrow K^0 \pi^-$ (right) events. Points with error bars represent data with $\mathcal{F} > 0$, the open histogram is the fit result and the hatched histogram is the background. The straight line shows the $q\bar{q}$ continuum background contribution.

the comparison of the measurement of the coefficient of the CP -violating $\sin(\Delta m_d t)$ term in the time dependent analysis of neutral B meson decays. In $B^0 \rightarrow (c\bar{c})K^0$ decays [where $(c\bar{c})$ denotes a charmonium state] this coefficient is $\sin 2\phi_1$. Precise measurements of $\sin 2\phi_1$ (also referred to as $\sin 2\beta$) have recently been reported by the Belle and BaBar experiments [18]. The best known candidates for $b \rightarrow s$ penguin-dominated processes, where this quantity can be measured independently, are $B^0 \rightarrow \phi K^0$ and $B^0 \rightarrow \eta' K^0$ decays. However, the branching fractions for these decay modes are of order $10^{-6} - 10^{-5}$ (including secondary branching fractions) and very large numbers of B mesons are required to perform these measurements. This is especially true for the ϕK^0 final state. The large signal observed in the three-body $B^0 \rightarrow K_S^0 K^+ K^-$ decay mode, where the ϕK_S^0 two-body intermediate state gives a relatively small contribution [5,19], would significantly increase the available statistics if these events could be used. Two complications are involved: (i) the $b \rightarrow u$ tree contributions may introduce an additional weak phase in the $B^0 \rightarrow K_S^0 K^+ K^-$ amplitude and complicate the interpretation of any observed CP violation. The $b \rightarrow u$ contribution in $B^0 \rightarrow \phi K_S^0$ is expected to be negligible (since ϕ is almost a pure $s\bar{s}$ state), which is not necessarily the case for the three-body $K_S^0 K^+ K^-$ final state. (ii) In contrast to the ϕK_S^0 state, which has fixed CP -parity, the CP -parity of the three-body $K_S^0 K^+ K^-$ final state is not *a priori* known. If the fractions of CP -even and CP -odd components are comparable, the use of the $K_S^0 K^+ K^-$ decay mode in a CP analysis will be complicated. Although in this case an analysis of the proper time distribution would not be useful for CP violation measurement, the analysis of the time evolution of the Dalitz plot may still provide useful information on CP violation in the $K_S^0 K^+ K^-$ final state. In what follows we discuss the possibility of using the three-body $B^0 \rightarrow K_S^0 K^+ K^-$ decay mode for CP violation measurements [20,21].

The decays of B mesons to three-body Khh final states can be described by $b \rightarrow u$ tree-level spectator and b

$\rightarrow s(d)g$ one-loop penguin diagrams. Although electroweak penguins, $b \rightarrow u$ W -exchange, and annihilation diagrams can also contribute to these final states, they are expected to be much smaller and we neglect them in the following discussion. B meson decays to final states with odd numbers of kaons (s -quarks) are expected to proceed dominantly via the $b \rightarrow sg$ penguin transition since, for these states, the $b \rightarrow u$ tree contribution has an additional CKM suppression. In contrast, B decays to three-body final states with two kaons proceed via the $b \rightarrow u$ tree and $b \rightarrow dg$ penguin transitions with no $b \rightarrow sg$ penguin contribution. This allows us to make a rough estimate of the $b \rightarrow u$ tree contribution to final states with three kaons via the analysis of $KK\pi$ final states. This is illustrated for the $B^+ \rightarrow K^+ K^+ K^-$ decay in Fig. 6, where the dominant $b \rightarrow s$ penguin graph is shown in Fig. 6(a). The $b \rightarrow u$ tree graph [Fig. 6(b)] has an additional Cabibbo suppression from the $W^+ \rightarrow \bar{s}u$ vertex. The corresponding diagram without Cabibbo suppression ($W^+ \rightarrow \bar{d}u$) shown in Fig. 6(d) is expected to be the dominant contributor to the $K^+ K^- \pi^+$ final state. Assuming factorization, a quantitative estimate of the fraction of the $b \rightarrow u$ tree amplitude is then provided by the ratio

$$F \equiv \frac{|\mathcal{A}_{b \rightarrow u}^{KKK}|^2}{|\mathcal{A}_{\text{total}}^{KKK}|^2} \sim \frac{\mathcal{B}(B^+ \rightarrow K^+ K^- \pi^+)}{\mathcal{B}(B^+ \rightarrow K^+ K^+ K^-)} \times \left(\frac{f_K}{f_\pi}\right)^2 \times \tan^2 \theta_C, \quad (2)$$

where $\mathcal{A}_{\text{total}}^{KKK}$ is the total amplitude for the $B^+ \rightarrow K^+ K^+ K^-$ decay and $\mathcal{A}_{b \rightarrow u}^{KKK}$ is its $b \rightarrow u$ tree contribution. The $(f_K/f_\pi)^2$ factor, where $f_\pi = 131$ MeV and $f_K = 160$ MeV are the pion and kaon decay constants, respectively, takes into account corrections for SU(3) breaking effects in the factorization approximation. θ_C is the Cabibbo angle ($\sin \theta_C = 0.2205 \pm 0.0018$) [8]. Using the results for $B^+ \rightarrow K^+ K^- \pi^+$ and $B^+ \rightarrow K^+ K^+ K^-$ branching fractions from Table I, we obtain $F \approx 0.022 \pm 0.005$. Similarly, for B^0 decays to $K^0 K^+ K^-$ and $K^0 K^+ \pi^-$ final states we find $F \approx 0.023 \pm 0.013$ (< 0.037),

TABLE II. List of systematic errors (in percent) for the three-body branching fractions.

Source	$K^+ \pi^+ \pi^-$	$K^0 \pi^+ \pi^-$	$K^+ K^+ K^-$	$K^0 K^+ K^-$	$K^+ K^0 K_S^0$	$K^+ K^+ K_S^0$	$K_S^0 K_S^0 K_S^0$	$K^+ K^- \pi^+$	$K^0 K^+ \pi^-$	$K_S^0 K_S^0 \pi^+$	$K^- \pi^+ \pi^+$	$K^+ K^+ \pi^-$
$B \rightarrow D \pi, D \rightarrow K \pi$ Branching fractions	6.3	11.7	6.3	11.7	6.3	11.7	11.7	6.3	11.7	6.3	6.3	6.3
Eff. nonuniformity over the Dalitz plot	4.3	3.5	2.2	3.6	5.9	7.2	5.3	5.3	5.7	6.1	6.8	5.3
Signal yield extraction	4.9	3.6	2.1	5.6	4.8	7.6	6.8					
PID			4.0	4.0	2.0	2.0	2.0	2.0	2.0			2.0
K_S^0 reconstruction					3.5	7.0				3.5		
MC statistics	3.3	2.9	2.9	2.9	3.4	4.6	3.3	3.3	4.1	3.7	3.3	3.2
Total	9.6	13.1	8.6	14.3	11.2	17.9	11.4	13.8	10.1	9.8		9.1

where the value in brackets is obtained using the upper limit for the $B^0 \rightarrow K^0 K^+ \pi^-$ branching fraction. Thus, the contribution of the $b \rightarrow u$ tree transition is expected to be at the level of a few percent in branching fraction or at the level of 10–15 % in amplitude. In contrast to two-body decays, where the magnitude of the interference term depends only on the relative phase between two amplitudes, in three-body decay, for the interference term to be maximal not only must the relative phase between the two amplitudes be 0 (180) degrees at any point of the phase space, but these two amplitudes should also have identical behavior over the phase space. It seems unlikely that all these conditions will be satisfied since $b \rightarrow s$ penguin and $b \rightarrow u$ tree amplitudes are quite different in nature. We conclude that the above value is a rather conservative estimate of the $b \rightarrow u$ contribution.

Let us now consider the CP content of the $K_S^0 K^+ K^-$ state in neutral B decays. The CP -parity of the $K_S^0 K^+ K^-$ three-body system is $(-1)^{l'}$, where l' is the orbital angular momentum of the $K^+ K^-$ pair relative to the remaining neutral kaon. Since the total angular momentum of the $K^0 K^+ K^-$ system is zero, l' is equal to the relative orbital angular momentum, l , of the two charged kaons. Thus, the relative fraction of CP -even and CP -odd states in the $K_S^0 K^+ K^-$ final state is determined by a fraction of states with even and odd orbital angular momenta in the $K^+ K^-$ system. This fraction could be determined by amplitude analysis of the $B^0 \rightarrow K_S^0 K^+ K^-$ Dalitz plot. Such an analysis requires high statistics and cannot be performed with the available data. Instead, we use isospin relations between the different three-kaon final states to determine the relative fraction of CP -even and CP -odd states. Noting that the dominant $b \rightarrow sg$ penguin transition is an isospin conserving process, and neglecting the isospin violating $b \rightarrow u$ tree and $b \rightarrow dg$ penguin contributions, we can write the following relations:

$$\mathcal{B}(B^0 \rightarrow K^0 K^+ K^-) = \mathcal{B}(B^+ \rightarrow K^+ K^0 \bar{K}^0) \times \frac{\tau_{B^0}}{\tau_{B^+}}; \quad (3)$$

$$\mathcal{B}(B^0 \rightarrow K^0 K^0 \bar{K}^0) = \mathcal{B}(B^+ \rightarrow K^+ K^+ K^-) \times \frac{\tau_{B^0}}{\tau_{B^+}}, \quad (4)$$

where the factor $\tau_{B^+}/\tau_{B^0} = 1.091 \pm 0.023 \pm 0.014$ [22] takes into account the difference in total widths of charged and neutral B mesons. Being a mirror reflection of each other in isospin space, $B^0 \rightarrow K^0 K^+ K^-$ and $B^+ \rightarrow K^+ K^0 \bar{K}^0$ decays should have not only equal partial widths [Eq. (3)], but also the same decay dynamics; specifically, the fraction of a certain angular momentum state in the $K^+ K^-$ system in the $K^0 K^+ K^-$ final state should be the same as that for the $K^0 \bar{K}^0$ system in the $K^+ K^0 \bar{K}^0$ final state. The $B^+ \rightarrow K^+ K^0 \bar{K}^0$ decay produces three different observable states: $K^+ K_S^0 K_S^0$, $K^+ K_L^0 K_L^0$ and $K^+ K_S^0 K_L^0$. The relative fractions of these states depend on the relative fractions of even and odd orbital angular momentum states in the $K^0 \bar{K}^0$ system. Bose statistics requires that the $K^0 \bar{K}^0$ wave function be symmetric (and, therefore, CP -even), independently of the relative or-

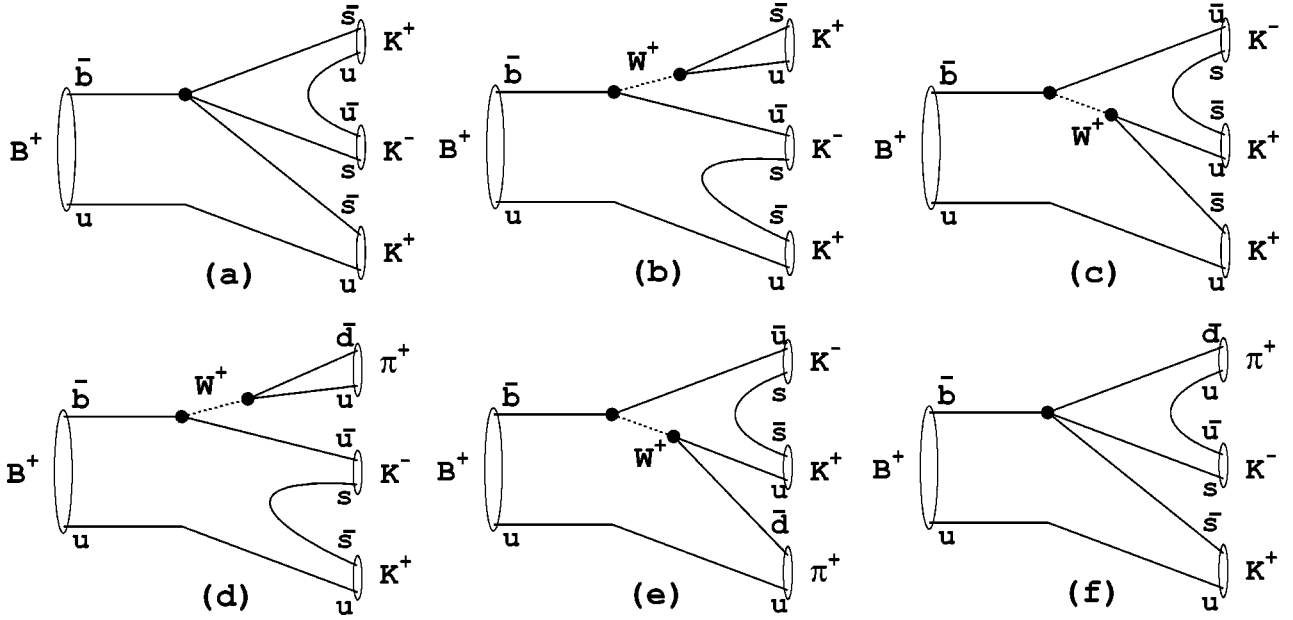


FIG. 6. Diagrams for $B^+ \rightarrow K^+ K^+ K^-$ decay: (a) $b \rightarrow s$ penguin; (b) and (c) $b \rightarrow u$ trees, and for $B^+ \rightarrow K^+ K^- \pi^+$ decay: (d) and (e) $b \rightarrow u$ trees; (f) $b \rightarrow d$ penguin.

total angular momentum, l , in the system of neutral kaons. As a result, a $K^0 \bar{K}^0$ system with l -even can only decay to $K_S^0 K_S^0$ or $K_L^0 K_L^0$ final states (with equal fractions), while a $K^0 \bar{K}^0$ system with l -odd can only decay to the $K_S^0 K_L^0$ final state (with an accuracy up to CP violation effects in the system of neutral kaons).

In this analysis we reconstruct only the $K^+ K_S^0 K_S^0$ component of the $K^+ K^0 \bar{K}^0$ final state. Measuring the $B^0 \rightarrow K^0 K^+ K^-$ and $B^+ \rightarrow K^+ K_S^0 K_S^0$ branching fractions and using the isospin relation (3) we can determine the parameter α^2 ,

$$\alpha^2 = 2 \frac{\mathcal{B}(B^+ \rightarrow K^+ K_S^0 K_S^0)}{\mathcal{B}(B^0 \rightarrow K^0 K^+ K^-)} \times \frac{\tau_{B^0}}{\tau_{B^+}} = \frac{N_{K^+ K_S^0 K_S^0}}{N_{K^0 K^+ K^-}} \times 2 \frac{\varepsilon_{K^0 K^+ K^-}}{\varepsilon_{K^+ K_S^0 K_S^0}} \times \frac{\tau_{B^0}}{\tau_{B^+}}. \quad (5)$$

Here, α^2 characterizes the fraction of states with even orbital angular momenta in the $K^0 \bar{K}^0$ system in the three-body $K^+ K^0 \bar{K}^0$ final state. Due to isospin symmetry it also gives the fraction of states with even angular momenta in the $K^+ K^-$ system for the $K_S^0 K^+ K^-$ final state. With the results given in Table I, we obtain $\alpha^2 = 0.86 \pm 0.15 \pm 0.05$, where we use the expression for α^2 in terms of signal yields (N) and reconstruction efficiencies (ε) instead of branching fractions to reduce the systematic error due to uncertainty in branching fractions of the calibration modes. Note that the $K_S^0 K^+ K^-$ final state includes the ϕK_S^0 state which is CP -odd. We remove $B^0 \rightarrow \phi K_S^0$ events by requiring $|M(K^+ K^-) - M_\phi| > 15 \text{ MeV}/c^2$; the number of remaining $K_S^0 K^+ K^-$ events is 123 ± 14 . The α^2 value for the remaining events is $\alpha_{\text{non } \phi}^2$

$= 1.04 \pm 0.19 \pm 0.06$. The fact that the $\alpha_{\text{non } \phi}^2$ value is close to unity provides evidence for the dominance of the CP -even component in the three-body $K_S^0 K^+ K^-$ final state when the ϕK_S^0 intermediate state is excluded.

From this analysis we conclude that the three-body $B^0 \rightarrow K_S^0 K^+ K^-$ decay can be useful for the measurement of CP violation in $b \rightarrow sg$ penguin dominated decays. Measurements of the time-dependent CP asymmetry in the $b \rightarrow sg$ penguin dominated $B^0 \rightarrow \eta' K_S^0$, $B^0 \rightarrow \phi K_S^0$ and $B^0 \rightarrow K_S^0 K^+ K^-$ decays are reported in Ref. [23].

X. CONCLUSION

In conclusion, we have measured branching fractions for charmless B meson decays to the $K^+ \pi^+ \pi^-$, $K^0 \pi^+ \pi^-$ and three-kaon $K^+ K^+ K^-$, $K^0 K^+ K^-$, $K^+ K_S^0 K_S^0$ and $K_S^0 K_S^0 K_S^0$ final states. We also observe 4σ evidence for the signal in the $K^+ K^- \pi^+$ final state that is expected to be dominated by the $b \rightarrow u$ tree transition. We do not see any signal in $B^+ \rightarrow K^- \pi^+ \pi^+$, $B^+ \rightarrow K^+ K^+ \pi^-$, $B^0 \rightarrow K^0 K^+ \pi^-$ and $B^+ \rightarrow K_S^0 K_S^0 \pi^+$ decays and present 90% C.L. upper limit for their branching fractions. All the results on three-body branching fractions are summarized in Table I. The results presented in this work are in good agreement with our previous measurements [5] and with those reported by the Ba-Bar [6] and CLEO [7] experiments. This paper does not update the results for quasi-two-body states obtained using the simplified technique in our previous analysis [5] because of the large model error of this technique. The extraction of branching fractions for exclusive quasi-two-body intermediate states in the observed three-body signals requires a full amplitude analysis of the corresponding Dalitz plots and is currently in progress.

An isospin analysis of the charmless B meson decays to

three-kaon final states suggests the dominance of the CP -even component in the three-body $K_S^0 K^+ K^-$ final state when the ϕK_S^0 intermediate state is removed. Using this final state increases the statistics available for measurements of CP violation in $b \rightarrow s$ penguin dominated decays by a factor of four compared to $B^0 \rightarrow \phi K_S^0$.

ACKNOWLEDGMENTS

We wish to thank the KEKB accelerator group for the excellent operation of the KEKB accelerator. We are grateful to V. Chernyak for fruitful discussions on the theoretical aspects of the analysis. We acknowledge support from the Min-

istry of Education, Culture, Sports, Science, and Technology of Japan and the Japan Society for the Promotion of Science; the Australian Research Council and the Australian Department of Education, Science and Training; the National Science Foundation of China under Contract No. 10175071; the Department of Science and Technology of India; the BK21 program of the Ministry of Education of Korea and the CHEP SRC program of the Korea Science and Engineering Foundation; the Polish State Committee for Scientific Research under Contract No. 2P03B 01324; the Ministry of Science and Technology of the Russian Federation; the Ministry of Education, Science and Sport of the Republic of Slovenia; the National Science Council and the Ministry of Education of Taiwan; and the U.S. Department of Energy.

-
- [1] N.G. Deshpande, N. Sinha, and R. Sinha, Phys. Rev. Lett. **90**, 061802 (2003).
 - [2] K. Huitu, C.D. Lu, P. Singer, and D.X. Zhang, Phys. Rev. Lett. **81**, 4313 (1998).
 - [3] K. Huitu, C.D. Lu, P. Singer, and D.X. Zhang, Phys. Lett. B **445**, 394 (1999).
 - [4] S. Fajfer and P. Singer, Phys. Rev. D **62**, 117702 (2000); **65**, 017301 (2002).
 - [5] Belle Collaboration, A. Garmash *et al.*, Phys. Rev. D **65**, 092005 (2002).
 - [6] BaBar Collaboration, B. Aubert *et al.*, hep-ex/0206004.
 - [7] CLEO Collaboration, E. Eckhart *et al.*, Phys. Rev. Lett. **89**, 251801 (2002).
 - [8] Particle Data Group, K. Hagiwara *et al.*, Phys. Rev. D **66**, 010001 (2002); and 2003 off-year partial update for the 2004 edition (<http://pdg.lbl.gov>).
 - [9] S. Kurokawa, Nucl. Instrum. Methods Phys. Res. A **499**, 1 (2003).
 - [10] Belle Collaboration, A. Abashian *et al.*, Nucl. Instrum. Methods Phys. Res. A **479**, 117 (2002).
 - [11] R. Brun *et al.*, GEANT 3.21, CERN Report DD/EE/84-1, 1984.
 - [12] R.A. Fisher, Ann. Geophys. (Germany) **7**, 179 (1936); M.G. Kendall and A. Stuart, *The Advanced Theory of Statistics*, 2nd ed. (Hafner, New York, 1968), Vol. III.
 - [13] CLEO Collaboration, D.M. Asner *et al.*, Phys. Rev. D **53**, 1039 (1996).
 - [14] Events are generated with the CLEO group's QQ program (<http://www.lns.cornell.edu/public/CLEO/soft/qq>).
 - [15] For $J/\psi(\psi(2S))$ rejection, we use the muon mass hypothesis to calculate the invariant mass of the two tracks.
 - [16] ARGUS Collaboration, H. Albrecht *et al.*, Phys. Lett. B **229**, 304 (1989).
 - [17] For the $K^- \pi^+ \pi^+$, $K^+ K^+ \pi^-$, and $K_S^0 K_S^0 \pi^+$ modes, we treat the fit result as a Gaussian measurement and quote 90% C.L. upper limits using the procedure of G.J. Feldman and R.D. Cousins, Phys. Rev. D **57**, 3873 (1998). For $K_S^0 K^+ \pi^-$, we quote only the upper edge of the Feldman-Cousins interval: this corresponds to an upper limit of confidence level greater than 90%. For the $K^+ K^- \pi^+$ mode, where we observe a 4σ signal, we quote $\mu + 1.28\sigma$, where μ and σ are the central value and the error returned by the fit.
 - [18] Belle Collaboration, K. Abe *et al.*, Phys. Rev. D **66**, 071102(R) (2002); BaBar Collaboration, B. Aubert *et al.*, Phys. Rev. Lett. **89**, 201802 (2002).
 - [19] BaBar Collaboration, B. Aubert *et al.*, Phys. Rev. Lett. **87**, 151801 (2001); Belle Collaboration, K.-F. Chen *et al.*, *ibid.* **91**, 201801 (2003).
 - [20] Belle Collaboration, K. Abe *et al.*, hep-ex/0208030.
 - [21] At the time of the preparation of this manuscript, papers by Y. Grossman, Z. Ligeti, Y. Nir, and H. Quinn, Phys. Rev. D **68**, 015004 (2003); and by M. Gronau and J.L. Rosner Phys. Lett. B **564**, 90 (2003) appeared that present more general formulations for isospin analyses of three kaon final states.
 - [22] Belle Collaboration, K. Abe *et al.*, Phys. Rev. Lett. **88**, 171801 (2002).
 - [23] Belle Collaboration, K. Abe *et al.*, Phys. Rev. D **67**, 031102(R) (2003).